Dalton Transactions

Accepted Manuscript

ROYAL SOCIETY OF CHEMISTRY

www.rsc.org/dalton

Dalton Transactions

RSCPublishing

ARTICLE

Room temperature high sensitive H_2S gas sensor based on SnO_2 multi-tubes arrays bio-templated from insect bristles

Cite this: DOI: 10.1039/xoxxoooooox

Received ooth January 2012,
Accepted ooth January 2012

DOI: 10.1039/xoxxoooooox

www.rsc.org/

Junlong Tian,[a] Feng Pan,[a] Ruiyang Xue,[a] Wang Zhang,[a*] Xiaotian Fang,[a] Qinglei Liu,[a] Yuhua Wang[b], Zhijian Zhang[c] and Di Zhang [a*]

A tin oxide multi-tubes arrays (SMTA) with a parallel effect was fabricated through a simple and promising method that combines chemosynthesis with biomimetic techniques which the biomimetic template derived from the bristles on the wings of the *Alpine Black Swallowtail* butterfly (Papilio maackii). The SnO_2 tubes are hollow and porous structure with micro-pores regularly distributed on the wall. The morphology, delicate microstructure and the crystal structure of this SMTA were characterized by super resolution digital microscope, scanning electron microscope, transmission electron microscope and X-ray diffraction. The SMTA exhibit a high sensitivity for H_2S gas at room temperature. It also exhibits a short response/recovery time, with an average value of 14/30 s at 5 ppm. Especially, it does not need to heat for the SMTA under the gas sensitivity measure process. On the basis of these results, SMTN is proposed as a suitable new material for the design and fabrication of room-temperature H_2S gas sensors.

1. Introduction

Hydrogen sulfide (H_2S) is a toxic gas[1, 2] that is often generated by organic waste, or as a byproduct of the oil and food industry. Its low threshold limit for humans of 20 ppb[3, 4] means that there is a very real need for gas sensor materials that can be used to fabricate an electronic nose which can help ensure public safety. Of the materials currently available, the 3.6 eV band gap of the n-type semiconductor tin oxide (SnO_2) has been extensively studied and applied in the field of gas sensors.[5-7] Through this, SnO_2 has been successfully applied to the detection of a number of different gases, such as CO, SO_2, NO_x, CH_4, and H_2S.[8] However, work is still needed to improve it sensitivity, as well as improving its temperature stability. In addition, most gas sensing detections of the sensing materials (not only for SnO_2) were performed under the operating temperature needed heating the sensing material.[6, 7, 9-13]

In principle, gas sensing by SnO_2 (semiconducting metal oxide) is based on the semiconductor surface, which causes a significant resistance change in proportion to the gas concentration and a certain work temperature.[14-16] In addition, the sensor performance depends on the doping or surface modification, exposed crystal planes, grain size, surface morphology, the working temperature, and so on. However, although doping or mixing is an efficient way to improve the sensor properties of SnO_2,[17, 18] the methods to make the materials homogeneous are too difficult to control[3, 19, 20] (i.e. reactive sputtering, pulsed laser deposition, electrochemical deposition). Encouragingly, along with the development of nanomaterials technology, the nanomaterials gas sensors with various morphologies were fabricated showed an excellent performance for gas sensing due to the small size effect[21] and a high absorption surface area[11, 13, 18]. Preparing SnO_2 with nano- or micro-sized structure materials become another method to improve the gas sensor properties.[22-27] Many researches made some progresses and innovations in fabricating SnO_2 nanotubes[28-30], due to the nanotubes or micro-tubes with high surface-to-volume ratios displayed enhanced and unexpected responses to the chemical molecules. But, limited by the currently technologies, it is difficult to fabricate the more effective nanomaterials gas sensors with more effective sub-micron functional morphologies.

Based on our previous work that a gas sensor was fabricated by single bio-inspired architectures porous micro-tube,[31] in this work, we combined the chemosynthesis with biomimetic techniques to assemble inorganic nanomaterials into multi-tubes arrays, which achieved the integration among the small size effect of the nanomaterials, the bio-inspired sub-micron architectures porous micro-tubes arrays with a high absorption surface area and parallel effect of the multi-tubes arrays. The biomimetic template derives from the bristles on the wings of the *Alpine Black Swallowtail* butterfly (ABSB) (Papilio maackii). The resultant SnO_2 multi-tubes array (SMTA) exhibits a high sensitivity for H_2S gas at room temperature and a short response/recovery time. Here, the first report on a H_2S gas sensor fabricated by singe component SnO_2 without any doping or composite, which does not need to heat for the SMTA under the gas sensitivity measure process, is presented. The method is facile and low-cost compared to other traditional techniques, and the fabrication process is very simple and easy

for practical applications. Especially, it does not need to heat for the SMTA under the gas sensitivity measure process, which exhibits a more obvious advantages for practical applications. Consequently, this work presents new insight to take advantage of the SnO_2 to fabricate the room temperature H_2S gas sensor.

2. Experimental section

2.1 preparation of SMTA

The method to fabricate the MTA was modified with our previous work.[31] Fig. 1 illustrates the strategy employed for fabricating the SMTA. The fabrication route escribed herein consists of three steps: 1) Pretreatment of the chitin-matrix surface; 2) After the same pretreatment with our previous work,[31] the bristles were dipped in prepared $SnCl_2$ ethanol solution for 36 hours at 30 ºC in sealed vessel; 3) Afterwards, the bristles were dried and heated in muffle furnace by the rate of 1 ºC/min to 550 ºC and kept for 2 hours (the chitin were burned off and left with crystallized SnO_2). Then, the SnO_2 bristles were cooled down to room temperature. Fig. 1 also exhibits that the sub-micron architectures porous micro-tube structure (SAPTS) was inherited and the structures of the bristles of ABSB were perfectly transferred to the SnO_2 bristles.

2.2 preparation of SMTA gas sensor

About 100 SnO_2 bristles as a parallel array that were in good condition were chosen, and then putted them together by a small needle. Following, painted silver paste onto the both ends of the SnO_2 bristles under the microscope as electrodes without any treatment. Finally, the samples were put in dried room (humility was under 70%) at 20 ºC.

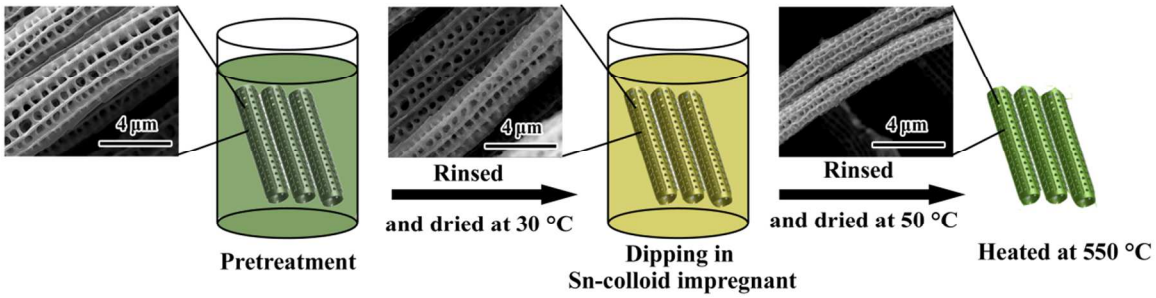

Fig. 1 Schematic view of the fabrication SMTA.

2.3 Material characterization techniques and measurements

SnO_2 microtubes were characterized by X-ray diffraction (XRD, Rigaku Dmax-2600/pc, Cu K radiation, λ = 0.1542 nm, 40 KV, 150 mA). The microstructure and morphology of the resultant products were investigated by field-emission scanning electron microscope (SEM) which was operated under 5.0 kV (Acc.V). Transmission electron microscope (TEM) images, selected area electron diffraction (SAED) patterns and high resolution transmission electron microscope (HRTEM) were obtained on a JEOL JEM-2100F instrument operated at an acceleration voltage of 200 KV (Acc.V).

The gas-sensing properties test was operated in a commercial measuring system of HW-30A (Hanwei Electronics Co., Ltd., China) and the details of testing measurement is also showed in a current paper.[11, 17, 32] The circuit voltage (V_c) was set at 5 V, and the output voltage (V_{out}) as the terminal voltage of the load resistor. The working temperature of a sensor was at room temperature (25 ºC). The gas response of the sensor (S) in this paper was defined as R_a/R_g, where R_a is the resistance in air and R_g is the resistance in sample gas for reducing gases. The response or recovery time was expressed as the time taken for the sensor output to reach 90% of its saturation after applying or switching off the gas in a step function. It does not need to heat for the SMTA under the gas sensitivity measure process.

3. Results and discussion

Fig. 2(a) is the SEM images of the SMTA gas sensor, which exhibits that the main component of the multi-tubes is approximate parallel and forms the multi-tubes arrays. Both ends of the SnO_2 multi-tubes were painted with silver paste as electrodes. Consequently, the SnO_2 multi-tubes combine with silver electrodes formed an approximate parallel circuit. As shown in Fig. 2(b) and (c), the quasi-order pores and longitudinal ridges are regularly distributed on the wall of the SnO_2 tubes. From the inset of Fig. 2(c), we can observe that the longitudinal center hole and microribs also are inherited. These figures also clearly show that the SnO_2 nanoparticles (NPs) deposited onto the surface and assembled into a film that successfully inherited the SAPTS of the bristle of ABSB.

Dalton Transactions RSCPublishing

ARTICLE

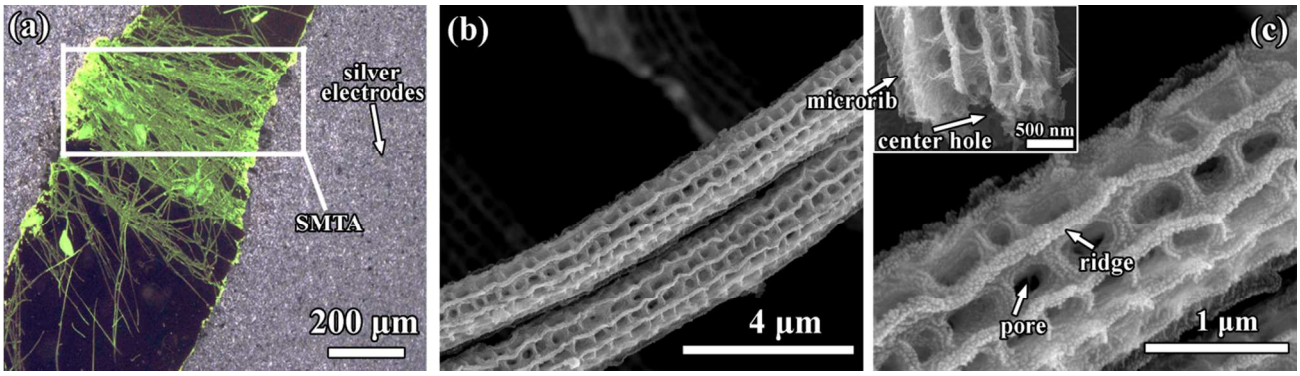

Fig. 2 (a) SEM images of the SMTA gas sensor. (b) and (c) SEM images of the SnO_2 microtubes. The inset of Fig. 2(c) is the cross-section images of the SnO_2 microtube.

Further observation was made under TEM (Fig. 3(a)-(d)). Fig. 3(a) and (b) also shows the morphology of porous wall. The SAED pattern demonstrates the polycrystalline of SnO_2, and rings indexed to (211), (110), (101) and (310) crystal planes, respectively. Moreover, SnO_2 NPs are attached to the wall of porous microtubes (Fig. 3(c)), which provides further supporting evidence that the SnO_2 NPs deposited onto the surface of the SAPTS of the bristle of ABSB. The HRTEM images of SnO_2 microtube (Fig. 3(d)) obviously exhibits that the NPs, which deposited on the surface of the SAPTS of the bristle of ABSB, are SnO_2 NPs. The lattice fringes with interplanar distance of $d_{SnO_2(110)} = 0.331nm$ and $d_{SnO_2(101)} = 0.263nm$ are exhibited in Fig. 3(d). The results of XRD (Fig. 3(e)) shows that all the diffraction peak of the powders is matched to the standard tin oxide, PDF card (#41-1445), which demonstrate that the NPs are tetragonal phase SnO_2, and the lattice parameters are marked. The clear rings of the SAED image match well with the XRD result.

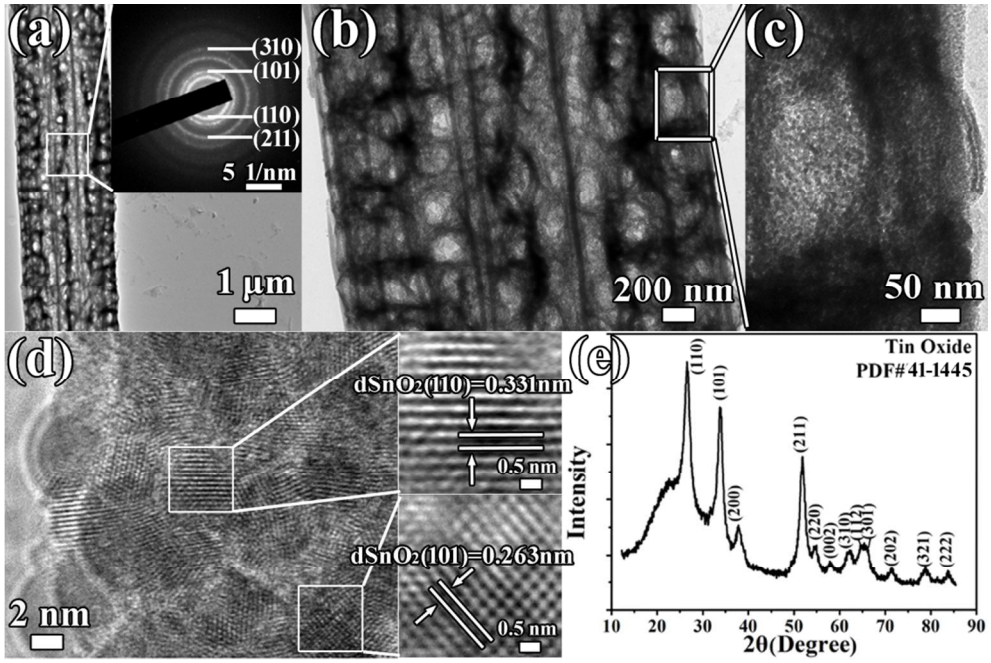

Fig. 3 (a)-(c) TEM images of SnO_2 microtube. The inset of Fig. 1(a) is the SAED image. (d) The HRTEM images of SnO_2 microtube. (e) XRD pattern of SnO_2 microtube.

Dalton Transactions RSCPublishing

ARTICLE

The SMTA showed high sensitivity for H_2S gases at room temperature (Fig. 4(a)), and V_{out} was showed as a function of time. When we tested reducing gases (H_2S), the load resistance was set as 4700 kΩ. As shown in Fig. 4(a), the sensor showed a significant response, when H_2S (100 ppm) was injected into the tested chamber. The response to H_2S was extremely high, the response time was below 10 s, and the recovery time was almost 40 s. Under the gas sensitivity measure process, it does not need to heat for the SMTA. The resistances changes are also significant when different concentrations (5, 10, 30, 50 and 100 ppm) H_2S was injected was injected (Fig. 4(b)). The S in 100 ppm H_2S is 5.21 and the high selectivity of H_2S gas sensor which would be useful in making a device to detect H_2S at room temperature without any heating device.

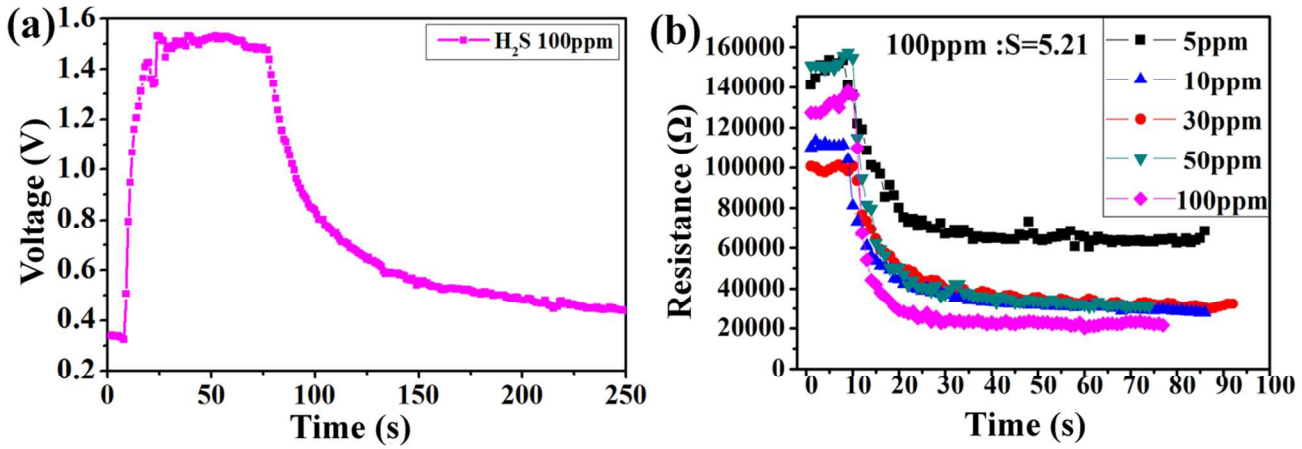

Fig. 4 (a) The V_{out} response and recovery curve of SMTA in 100 ppm H_2S gases. (b) The resistances change of SMTA in different concentrations (5, 10, 30, 50 and 100 ppm) H_2S.

Further experiments show the sensitivity of the SMTA precisely. The dynamic electrical response of the SMTA to different concentration of H_2S gas (from 5ppm to 50 ppm) is shown in Fig. 5(a), which shows the behaviour of the voltage signal (response) as a function of the time. As the H_2S gases with different concentrations were injected into the tested chamber, the response of gas sensor rapidly increased. After gas off, the response can almost recover to its initial value, rapidly. The result demonstrates that the H_2S gas sensor based on the SMTA possesses a good reversibility. Even in 5 ppm H_2S, the sensor also show a response time about 14 s and recovery time was 30 s. The high sensitivity and short response/recovery time are much better than many other H_2S gas-sensing SnO_2 microtubes reported previously.[28, 30, 33] The sensor exhibits high response to thin H_2S and the response increase rapidly with the growth of the gas concentration. The relative resistance is defined as R_a/R_g (Fig. 5(b)), and the $S_i=\Delta R/\Delta C$ is defined as the sensitivity when concentration increased, where ΔR represents R_a/R_g. The sensors also showed obvious changes when concentration changed. The high density of bristles amplified the signal of H_2S, and the S was ~4.84×10^{-2}, which was 3 times more than some other tubes.[30]

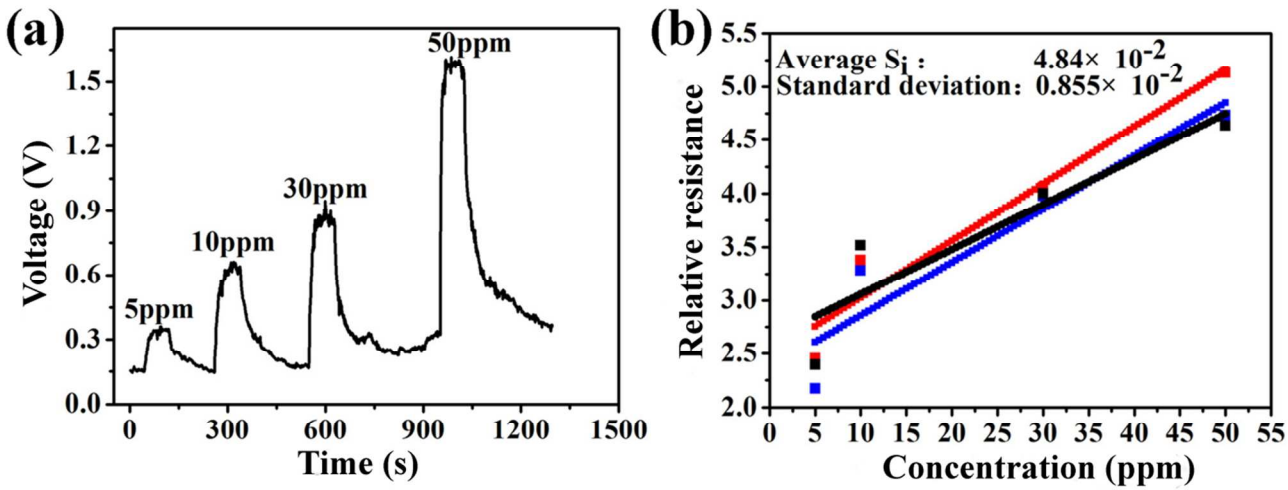

Fig. 5 (a) V_{out} of SMTA in different concentrations (5, 10, 30 and 50 ppm) of H_2S; (b) relative resistance response of SMTA in different concentrations (5, 10, 30 and 50 ppm) of H_2S (three different colors represent to three different batches of samples with same process).

Table 1 shows a development in gas sensors of nanotubes or microtubes made by tin oxide in recent five years. This table shows that the SMTA with the SAPTS has significantly improved the gas sensor properties in H_2S. Many researchers before used heating, doping or compositing as the methods to improve the sensitivity of gas sensors, the operating temperature was usually over 100 **ºC**.[4, 9, 19, 34] Unlike those sensors, the SMTA gas sensors with SAPTS also have an excellent sensitivity at room temperature, reducing the operating costs and hardware bulk, while improving the device reliability through the simplification of the operating requirements. Moreover, the sensor shows a good response low to 5 ppm. Although some reports have shown really low concentration (even down to ppb level) detection for H_2S gas sensors,[35, 36] the response and recovery time to H_2S are longer at room temperature due to the low operating temperature, which are difficult to be fabricated and to be widely used in practical application. However, the SMTA gas sensors with high sensitivity and short response/recovery time could be easily fabricated and in good use in the detection of H_2S.

Table 1 Summary of the development of gas sensors of H_2S based on SnO_2 microtubes (R-T, room temperature).

Years	Low detection limit (ppm)	Response time	Recovery time	Operating temperature (ºC)	Sensor response (S)
2011[28]	~20	~10 min	~1 min	30-90	0.35
2013[37]	~0.5	＞10 min	＞10 min	R-T	＜0.1
2014[30]	~9	~30 s	~30 s	R-T	~1
This work	~5	~14 s	~30 s	R-T	~1.45

We now turn to discussion of the dynamic electrical response of the SMTA to H_2S gas, referring to the scheme of Fig. 6. The dynamic electrical response on the SMTA commonly involves the interaction between H_2S gas and the chemisorbed oxygen ions on the surface. In ambient air, there is a lot of chemisorbed oxygen $O_2^-(ads)$ on the SMTA surface at room temperature, and electrons from SnO_2 are trapped by chemisorbed oxygen species, as shown in Eqs. (1) and (2).[18, 38]

$$O_2(g) \Leftrightarrow O_2(ads) \quad (1)$$

$$O_2(ads) + e^- \rightarrow O_2^-(ads) \quad (2)$$

Thereupon, the chemisorbed oxygen causes electron depletion formed a space-charge layer in the SMTA surface and results in the building up of a Schottky surface barrier, which results in the electrical conductance of the SMTA decreased to a minimum.[38] When injected into H_2S gas the tested chamber, the chemisorbed oxygen $O_2^-(ads)$ react with H_2S gas, and the response to H_2S at room temperature can be explained as Eqs. (3).[18]

$$H_2S(g) + \frac{3}{2}O_2^-(ads) \rightarrow H_2O(g) + SO_2(g) + \frac{3}{2}e \quad (3)$$

With this reaction, many extracted electrons are released to the SMTA surface, leading to the Schottky surface barrier decrease and the space-charge layer thinner. Therefore, the electrical conductivity of SMTA increases. Consequently, the chemisorbed oxygen causes the electrical conductance of the SMTA decreased and the chemisorbed reducing gas causes the electrical conductivity of SMTA increased which resulted in the dynamic electrical response of the SMTA to H_2S gas. For SMTA, the H_2S gas sensor exhibits high response, firstly, the crystallite size should be comparable to 2 L_d (the thickness of surface electron depletion layer denotes L_d). For SnO_2 in air, L_d is about 3 nm.[21] From the TME results and the XRD results (Fig. 3), we can find that the SnO_2 grains are high crystalline and the sizes are about 7.0 nm. Moreover, the SAPTS of SnO_2

micro-tube bio-templated from ABSB with quasi-order pores regularly distributed on the wall and a longitudinal center hole located in the center of the micro-rib. These structures provide lots of channels to facilitate the H_2S gas diffusion into such the SAPTS, making the H_2S gas contact with inner SnO_2 grain easily on the reduction reaction process and degas easily on the recovery process. The SAPTS provide abundant gas absorption surface, and more gas would be absorbed at relatively low temperature which cause that the H_2S gas sensitivity was enhanced and the sensing temperature zone was moved to room temperature.[18] Consequently, the SAPTS also play a crucial role on the fast response/recovery. Simultaneously, the high crystalline framework[11] and the longitudinal ridges structure provide fast transport of charge carriers from one end of micro-tube to other end. In addition, the multi-tubes are approximate parallel formed parallel circuit which reduces the resistance compared with single tube and facilitates dynamic electrical response. Hence, the resultant SMTA exhibits a high sensitivity for H_2S gas at room temperature and a short response/recovery time.

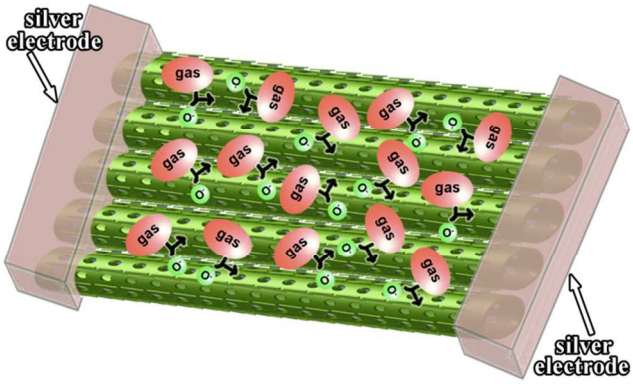

Fig. 6 Schematic of the SMTA gas sensors which generates response as the H_2S gases were injected into the tested chamber

Conclusions

In this work, we fabricate the SMTA with SAPTS through a simple and promising method that combines chemosynthesis with biomimetic techniques. The biomimetic template derived from the bristles on the wings of the *Alpine Black Swallowtail* butterfly. The SMTA with electrodes contacted on two ends was assembled into the gas sensor devices. Due to the high crystalline small size SnO_2 grain integrated with the SAPTS, as well as combined with the parallel effect of the multi-tubes arrays, the SMTA H_2S gas sensor exhibits a high sensitivity for H_2S gas at room temperature and a short response/recovery time. All of these properties indicate that the SMTA has the potential that could be applied to make devices, which could detect H_2S at room temperature to ensure the safety of human and animals. And this work opens a novel way to fabricate the room temperature gas sensor.

Acknowledgements

This work was supported by the National Natural Science Foundation of China (no.51202145 and no. 51271116), the National Basic Research Program of China (973 Program, no. 2011cb922200), Shanghai Science and Technology Committee (15ZR1422400, 14JC1403300, 14520710100) and Research Fund for the Doctoral Program of Higher Education of China (20120073120006 and 20120073130001)

Notes and references

[a] State Key Laboratory of Metal Matrix Composites, Shanghai Jiao Tong University, 800 Dongchuan Road, Shanghai, 200240, P. R. China.
[b] Department of Prosthodontics, Shanghai Jiao Tong University, 800 Dongchuan Road, Shanghai, 200240, P. R. China.
[c] Jushi Fiberglass Research Institute, Zhejiang Key Laboratory for Fiberglass Research, Jushi Group Co., Ltd., Zhejiang, 314500, P. R. China.
E-mail: wangzhang@sjtu.edu.cn; zhangdi@sjtu.edu.cn; Fax: +86-21-34202749; Tel: +86-21-34202634

1. M. Whiteman, N. S. Cheung, Y.-Z. Zhu, S. H. Chu, J. L. Siau, B. S. Wong, J. S. Armstrong and P. K. Moore, *Biochem. Biophys. Res. Commun.*, 2005, **326**, 794-798.
2. I. R. I. System, Toxicological review of hydrogen sulphide. http://www.epa.gov/iris/, 2003.
3. J.-H. Jeun, D.-H. Kim and S.-H. Hong, *Mater. Lett.*, 2013, **105**, 58-61.
4. J. Tamaki, K. Shimanoe, Y. Yamada, Y. Yamamoto, N. Miura and N. Yamazoe, *Sensors Actuators B: Chem.*, 1998, **49**, 121-125.
5. N. Barsan, M. Schweizer-Berberich and W. Göpel, *Fresenius J. Anal. Chem.*, 1999, **365**, 287-304.
6. Z. Li, Q. Zhao, W. Fan and J. Zhan, *Nanoscale*, 2011, **3**, 1646-1652.
7. H.-R. Kim, K.-I. Choi, K.-M. Kim, I.-D. Kim, G. Cao and J.-H. Lee, *Chem. Commun.*, 2010, **46**, 5061-5063.
8. G. Eranna, B. Joshi, D. Runthala and R. Gupta, *Crit. Rev. Solid State Mater. Sci.*, 2004, **29**, 111-188.
9. R. Vasiliev, M. Rumyantseva, N. Yakovlev and A. Gaskov, *Sensors Actuators B: Chem.*, 1998, **50**, 186-193.
10. Y. Zhang, Q. Xiang, J. Xu, P. Xu, Q. Pan and F. Li, *J. Mater. Chem.*, 2009, **19**, 4701-4706.
11. Y. Li, W. Luo, N. Qin, J. Dong, J. Wei, W. Li, S. Feng, J. Chen, J. Xu and A. A. Elzatahry, *Angew. Chem., Int. Ed.*, 2014, **53**, 9035-9040.
12. W. Qin, L. Xu, J. Song, R. Xing and H. Song, *Sensors & Actuators: B. Chem.*, 2013, **185**, 231-237.
13. S. Zhang, P. Zhang, Y. Wang, Y. Ma, J. Zhong and X. Sun, *ACS Appl. Mater. Interfaces*, 2014, **6**, 14975-14980.
14. A. PATRA and A. Kar, *J. Mater. Chem. C*, 2014.
15. G. W. Ho, *Sci. Adv. Mater.*, 2011, **3**, 150-168.
16. N. Yamazoe, *Sensors Actuators B: Chem.*, 2005, **108**, 2-14.
17. H. Wang, K. Dou, W. Y. Teoh, Y. Zhan, T. F. Hung, F. Zhang, J. Xu, R. Zhang and A. L. Rogach, *Adv. Funct. Mater.*, 2013, **23**, 4847-4853.
18. G. Fang, Z. Liu, C. Liu and K.-l. Yao, *Sensors Actuators B: Chem.*, 2000, **66**, 46-48.
19. M. Verma, A. Chowdhuri, K. Sreenivas and V. Gupta, *Thin Solid Films*, 2010, **518**, e181-e182.
20. A. Chowdhuri, S. K. Singh, K. Sreenivas and V. Gupta, *Sensors Actuators B: Chem.*, 2010, **145**, 155-166.
21. Y. Chen, L. Nie, X. Xue, Y. Wang and T. Wang, *Appl. Phys. Lett.*, 2006, **88**, 083105-083105-083103.
22. X. Xu, J. Zhuang and X. Wang, *J. Am. Chem. Soc.*, 2008, **130**, 12527-12535.
23. P. Sun, W. Zhao, Y. Cao, Y. Guan, Y. Sun and G. Lu, *CrystEngComm*, 2011, **13**, 3718-3724.

24. D. Hu, B. Han, S. Deng, Z. Feng, Y. Wang, J. Popovic, M. Nuskol, Y. Wang and I. Djerdj, *J. Phys. Chem. C*, 2014.
25. Q. Liu, Z. Zhenyu, W. Li, K. Xu, R. Zou and J. Hu, *CrystEngComm*, 2015.
26. W. Tan, X. Ruan, Q. Yu, Z. Yu and X. Huang, *Sensors*, 2014, **15**, 352-364.
27. F. Li, Y. Chen and J. Ma, *J. Mater. Chem. A*, 2014, **2**, 7175-7178.
28. H. Dai, P. Xiao and Q. Lou, *Phys. Status Solidi A*, 2011, **208**, 1714-1717.
29. Y. Zhang, S. Cui, J. Chang, L. E. Ocola and J. Chen, *Nanotechnology*, 2013, **24**, 025503.
30. F. Mendoza, D. M. Hernández, V. Makarov, E. Febus, B. R. Weiner and G. Morell, *Sensors Actuators B: Chem.*, 2014, **190**, 227-233.
31. W. Zhang, J. Tian, Y. a. Wang, X. Fang, Y. Huang, W. Chen, Q. Liu and D. Zhang, *J. Mater. Chem. A*, 2014, **2**, 4543-4550.
32. N. Qin, X. Wang, Q. Xiang and J. Xu, *Sensors Actuators B: Chem.*, 2014, **191**, 770-778.
33. S. Mubeen, M. Lai, T. Zhang, J.-H. Lim, A. Mulchandani, M. A. Deshusses and N. V. Myung, *Electrochim. Acta*, 2013, **92**, 484-490.
34. C. M. Ghimbeu, M. Lumbreras, M. Siadat, R. C. van Landschoot and J. Schoonman, *Sensors Actuators B: Chem.*, 2008, **133**, 694-698.
35. C. Wang, X. Chu and M. Wu, *Sensors Actuators B: Chem.*, 2006, **113**, 320-323.
36. M. Kaur, N. Jain, K. Sharma, S. Bhattacharya, M. Roy, A. Tyagi, S. Gupta and J. Yakhmi, *Sensors Actuators B: Chem.*, 2008, **133**, 456-461.
37. S. Mubeen, M. Lai, T. Zhang, J.-H. Lim, A. Mulchandani, M. A. Deshusses and N. V. Myung, *Electrochim. Acta*, 2013, **92**, 484-490.
38. F. Song, H. Su, J. Han, J. Xu and D. Zhang, *Sensors Actuators B: Chem.*, 2010, **145**, 39-45.

Table of contents entry

A tin oxide multi-tubes arrays with a parallel effect was fabricated, exhibited high sensitivity for H_2S gas at room temperature.